

A Novel RGD-independent Cell Adhesion Pathway Mediated by Fibronectin-bound Tissue Transglutaminase Rescues Cells from Anoikis*[§]

Received for publication, March 31, 2003

Published, JBC Papers in Press, May 5, 2003, DOI 10.1074/jbc.M303303200

Elisabetta A. M. Verderio[‡], Dilek Telci[‡], Afam Okoye[‡], Gerry Melino[§], and Martin Griffin[¶]

From the [‡]Department of Life Sciences, Nottingham Trent University, Clifton Lane, Nottingham NG11 8NS, United Kingdom, the [§]Department of Experimental and Biochemical Sciences, D26/F153, University of Rome "Tor Vergata," 00133 Rome, Italy, and the [¶]Medical Research Council, Toxicology Unit, Hodgkin Building, Leicester University, Leicester LE1 9HN, United Kingdom

Specific association of tissue transglutaminase (tTG) with matrix fibronectin (FN) results in the formation of an extracellular complex (tTG-FN) with distinct adhesive and pro-survival characteristics. tTG-FN supports RGD-independent cell adhesion of different cell types and the formation of distinctive RhoA-dependent focal adhesions following inhibition of integrin function by competitive RGD peptides and function blocking anti-integrin antibodies $\alpha_5\beta_1$. Association of tTG with its binding site on the 70-kDa amino-terminal FN fragment does not support this cell adhesion process, which seems to involve the entire FN molecule. RGD-independent cell adhesion to tTG-FN does not require transamidating activity, is mediated by the binding of tTG to cell-surface heparan sulfate chains, is dependent on the function of protein kinase C α , and leads to activation of the cell survival focal adhesion kinase. The tTG-FN complex can maintain cell viability of tTG-null mouse dermal fibroblasts when apoptosis is induced by inhibition of RGD-dependent adhesion (anoikis), suggesting an extracellular survival role for tTG. We propose a novel RGD-independent cell adhesion mechanism that promotes cell survival when the anti-apoptotic role mediated by RGD-dependent integrin function is reduced as in tissue injury, which is consistent with the externalization and binding of tTG to fibronectin following cell damage/stress.

Subtle changes in the extracellular matrix (ECM)¹ complexity/tissue architecture may be crucial for the regulation of the

* This work was supported in part by grants from Engineering and Physical Research Council (GR/L43688), Telethon (E872, E1224), Associazione Italiana per la Ricerca sul Cancro, European Commission, and Ministero dell'Istruzione dell'Università e della Ricerca. The costs of publication of this article were defrayed in part by the payment of page charges. This article must therefore be hereby marked "advertisement" in accordance with 18 U.S.C. Section 1734 solely to indicate this fact.

[§] The on-line version of this article (available at <http://www.jbc.org>) contains supplemental Fig. S1.

[¶] To whom correspondence should be addressed: Dept. of Life Sciences, Nottingham Trent University, Clifton Lane, Nottingham, NG11 8NS, UK. Tel.: 44-115-848-6670; Fax: 44-115-848-6636; E-mail: martin.griffin@ntu.ac.uk.

¹ The abbreviations used are: ECM, extracellular matrix; FN, fibronectin; HSPG, heparan sulfate proteoglycans; tTG, tissue transglutaminase; PKC α , protein kinase C α ; HOB, human osteoblasts; DMEM, Dulbecco's modified Eagle's medium; MDF, mouse dermal fibroblasts; TCP, tissue culture plastic; ELISA, enzyme-linked immunosorbent assay; PBS, phosphate-buffered saline; FITC, fluorescein isothiocyanate; tet, tetracycline; TdT, terminal deoxynucleotidyl transferase; TUNEL, TdT-mediated dUTP nick end labeling; XTT, 2,3-bis[2-methoxy-4-nitro-5-sulfophenyl]-2H-tetrazolium-5-carboxanilide; TCP, tissue culture plastic; DTT, dithiothreitol; FAK, focal adhesion kinase.

apoptotic machinery leading to anoikis (1, 2). Such a process occurs during tissue injury when the composition and integrity of the ECM are altered in several significant ways (3). A central component of the ECM, which regulates adhesion-dependent survival signaling, is the adhesive glycoprotein fibronectin (FN) (4). FN binds to cell-surface matrix receptors, primarily the $\alpha_5\beta_1$ integrins, through the Arg-Gly-Asp (RGD) cell-binding site within the Type III₁₀ domain. The importance of the RGD cell-binding domain in adhesion-mediated cell survival has been demonstrated by employing synthetic peptides containing the RGD motif, which induce apoptosis in many cell types, by acting as competitive inhibitors of FN-integrin interaction and activators of caspase 3 (5, 6). A comparable scenario may occur in wounding and inflammatory conditions, whereby fragmentation of FN can lead to detachment-induced apoptosis (5, 7). However, the RGD cell-binding domain of FN is not sufficient in isolation to regulate cell survival, which must be sustained by other critical FN domains such as the C-terminal heparin-binding domain (HepII) (7, 8), known to synergistically interact with heparan sulfate proteoglycans (HSPG) receptors and integrin $\alpha_4\beta_1$ (9). Evidence is also accumulating to suggest that changes in the molecular structure and composition of the FN matrix may provide new signals to regulate cell shape, migration, and proliferation. Alterations to the conformation of FN either by multimerization (10) or heterotypic association with other matrix molecules (11) could reveal biologically active neo-epitopes, which regulate cell responses via the induction of cytoskeleton assembly (12). Modulation of the FN matrix may therefore also be fundamental in the regulation of adhesion-related apoptosis.

One protein that binds with high affinity specialized FN domains and modulates the function of FN is tissue-type transglutaminase (tTG, TG-2) (10, 13, 14). tTG is a multifunctional protein implicated in diverse normal and pathological processes (15) but more specifically is regarded as an important component of cell/tissue defense in response to cell damage and stress (16, 17). tTG differs from the other transglutaminases in that the transamidase active site is integrated with a GTP binding/hydrolysis site, which negatively regulates the transamidation activity by structurally blocking the active site (18). Another peculiarity of tTG is its externalization into the ECM via a non-Golgi/endoplasmic reticulum route, through a mechanism that appears to depend on its active-state conformation (19) and an intact FN-binding site in the 28-kDa amino-terminal sandwich region (20, 21). Matrix deposition of tTG increases in situations of tissue damage and cellular stress and results in the immobilization of tTG on matrix FN (16, 17, 20, 22), which in turn protects tTG from matrix degradation (23). Consistent with these findings is the observation that guinea pig liver tTG forms specific complexes with human plasma FN,

and it appears as a globular protein bound to the N-terminal portion of FN interacting either with the Type I₄-I₅ motif (24) or with a sequence within the gelatin-binding domain of FN (I₆-II₁-II₂-I₇-I₈-I₉) (13).

The involvement of tTG in the adhesion of multiple cell types is now consolidated (25, 26); however, the molecular mechanism and its physiological significance remain controversial. It has been proposed that tTG enhances cell adhesion through matrix remodeling, via protein cross-linking (10, 26); however, recent findings suggest that tTG involvement in cell-matrix interactions is independent from its transamidation activity (19, 27, 28). Cell-surface tTG might act as an adhesion co-receptor of integrins β_1 and β_3 by mediating cell adhesion to the gelatin-binding domain of FN (27) or, conversely, act as an independent adhesion protein by specific binding to $\alpha_4\beta_1$ and $\alpha_9\beta_1$ integrins (28).

In the current study we have explored the involvement of tTG in FN-mediated cell survival, starting with the hypothesis that the ECM function of tTG is strictly dependent on its association with FN, and that tTG and FN reciprocally modulate each others functions following complex formation. We report that FN-bound tTG supports a novel RGD-independent cell adhesion process, which is mediated by the direct binding of tTG to the cell surface through a mechanism that is critically dependent on cell-surface heparan sulfate and activation of protein kinase C α (PKC α). We describe that FN-bound tTG, but not FN, can rescue tTG-deficient mouse dermal fibroblasts from apoptosis induced by inhibition of RGD-dependent cell adhesion (anoikis), with maintenance of cell viability. Our findings suggest that matrix FN with bound tTG is functionally distinct from either protein acting in isolation and suggest a novel RGD-independent pathway that may be important in cell survival under conditions of cell damage/stress.

EXPERIMENTAL PROCEDURES

Reagents and Antibodies—Mouse monoclonal antibodies included anti-integrin β_1 (JB1A) and α_5 (PID6) (Chemicon); vinculin and tubulin (Sigma-Aldrich); and tTG (Cub74) (NeoMarkers). Rabbit polyclonal antibodies included anti-human fibronectin (Sigma-Aldrich) and anti-human Tyr(p)³⁹⁷-FAK (Upstate Biotechnology). The tTG inhibitor R283 (19) was synthesized by R. Saint and I. Coutts, Nottingham Trent University. Purified guinea pig liver tTG was either obtained by Sigma-Aldrich or purified according to Leblanc *et al.* (29). Human plasma FN and FN proteolytic fragments, GTP γ -S, and synthetic RGD-specific peptides (GRGDTP and GRGDSP) were from Sigma-Aldrich and control RAD peptide (GRADSP) was from Calbiochem. Heparitinase (EC4.2.2.8) was from Sigma-Aldrich, and chondroitinase ABC (protease-free) from Seikagaku Corporation. The PKC α inhibitor GO6976 was from Calbiochem.

Cell Lines—Primary human osteoblasts (HOB) were provided by S. Downes (University of Nottingham, Nottingham, UK) and maintained in Dulbecco's modified Eagle's medium (DMEM) as we previously described (30). Swiss 3T3 albino fibroblasts were obtained from American Type Culture Collection and maintained in DMEM supplemented with 10% (v/v) fetal calf serum, 2 mM glutamine, and penicillin/streptomycin (100 units/ml and 100 μ g/ml, respectively). Transfected Swiss 3T3 fibroblasts, displaying inducible expression of tTG (clone TG3), were cultured and induced as described by Verderio *et al.* (22). Primary mouse dermal fibroblasts (MDF) were isolated from the skin of tTG-deficient (MDF-TG^{-/-}) and wild type (MDF-TG^{+/+}) 9-months-old mice and maintained as described by De Laurenzi and Melino (31).

Immobilization of TG on FN and Amino-terminal FN Fragments—96-well plates were coated with human plasma FN (5 μ g/ml) or with the 70 kDa (42 μ g/ml), 45 kDa (54 μ g/ml), and 30 kDa (54 μ g/ml) proteolytic fragments of FN in 50 mM Tris-HCl, pH 7.4, 50 μ l/well, by incubation at 4 °C for ~15 h. Concentrations of FN and FN fragments were optimal to saturate tissue culture plastic (TCP), as measured by an ELISA-based assay with polyclonal anti-FN antibody (1/5000) followed by peroxidase-labeled anti-rabbit IgG (1/5000). FN fragments were in a 30-, 60-, and 90-fold stoichiometric excess, respectively, of control FN. For tTG immobilization, the FN solution was removed, the wells were washed once in 50 mM Tris-HCl, pH 7.4, and then incubated with purified guinea pig

liver tTG (20 μ g/ml) in phosphate-buffered saline (PBS) containing 2 mM EDTA, 100 μ l/well. After 1 h at 37 °C, the tTG solution was removed and wells were washed once in 50 mM Tris-HCl, pH 7.4, and once in serum-free culture medium before cell seeding. In some experiments FN-coated plates were blocked with 3% (w/v) lipid milk protein (Marvel) in PBS at 37 °C for 30 min and then washed twice with 50 mM Tris-HCl, pH 7.4, prior to tTG immobilization. The presence of tTG immobilized on FN was confirmed by an ELISA-type assay using Cub74 as we previously described (26). The transamidation activity of the immobilized tTG was determined by the incorporation of biotinylated cadaverine into FN as previously described (26) and compared with the activity of free tTG standard. Data are expressed as absorbance 450 nm with 5 mM Ca²⁺ in the reaction buffer minus background absorbance values with 5 mM EDTA.

Cell Adhesion Assay—Exponentially growing cells were detached using 0.25% (w/v) trypsin in 5 mM EDTA, collected into medium containing a ~7% (v/v) fetal calf serum, washed twice with medium without fetal calf serum, and then plated onto 96-well plates (2 \times 10⁴ cells/well), coated with FN or FN fragments, with and without immobilized tTG. After a maximum of 20 min incubation (to minimize the secretion of any endogenous protein) at 37 °C in a 5% CO₂ atmosphere, cells were fixed in 3.7% (w/v) paraformaldehyde in PBS, permeabilized in 0.1% (v/v) Triton X-100 in PBS, and stained with May Grunwald and Giemsa stain (26). In some cases cells were pre-treated for 15 h with 1 mM cycloheximide before plating, to rule out any effects of endogenous secreted adhesion molecules. Digital images of 3 non-overlapping fields covering the central portion of each well were captured using a video digital camera (Olympus DP10) and examined using the Image Analysis program Scion Image (National Institute of Health). At least 9 images of separate fields per sample were examined for a total of at least 400 cells in the FN control. The number of attached cell particles in each field was measured by "thresholding" and "particle analysis" and the spread cells by "density slicing."

Cytoskeletal Staining—Actin stress fibers were visualized using fluorescein isothiocyanate (FITC)-labeled phalloidin and focal adhesions by staining for vinculin. Cells were seeded in 0.79-cm²-wells of chamber slides (8 \times 10⁴ cells/well) previously coated with FN and tTG-FN and allowed to adhere for ~20 min. Cells were fixed using 3.7% (w/v) paraformaldehyde in PBS and permeabilized in 0.1% (v/v) Triton X-100 in PBS. For actin stress fibers, cells were then blocked in PBS buffer supplemented with 5% (w/v) dry milk and then incubated with FITC-labeled phalloidin (20 μ g/ml) in blocking buffer. For localization of vinculin, cells were blocked in PBS buffer containing 3% (w/v) bovine serum albumin and then incubated with mouse monoclonal anti-vinculin antibody (1:100) in blocking buffer. Bound antibody was revealed by incubation with rabbit anti-mouse IgG-FITC (1:100) (Dako) in blocking buffer. Coverslips were mounted with Vectashield mountant containing propidium iodide (Vector Laboratories) and examined by laser confocal microscopy using a Leica TCSNT system (Leica Lasertechnik). Consecutive scanning sections (~2 μ m) from the upper to the lower attachment site of cells were overlaid as an extended focus image, and imaged cells (from at least 8 random fields, at least 100 cells in FN control) were scored for actin stress fiber formation with the aid of the Leica TCSNT (version 1.5–451) image processing menu.

Inhibition of Integrin-mediated Cell Adhesion—Cells in suspension (2 \times 10⁵ cells/ml) were incubated with GRGDTP synthetic peptide (32) (50 μ g/ml, ~75 μ M, 100 μ g/ml ~150 μ M, or 200 μ g/ml ~300 μ M). Some experiments were reproduced using the FN-prototype GRGDSP peptide. Alternatively, cells in suspension (2 \times 10⁵ cells/ml) were incubated with function blocking anti-integrin antibodies (JB1A, 40 μ g/ml; and PID6, 30 μ g/ml). All incubations were performed in serum-free medium at 37 °C for 10 min. Afterwards cells were seeded in the presence of either the competitive RGD peptides or the anti-integrin antibodies.

Cell Treatment with C3 Exotransferase—*Clostridium botulinum* C3 exotransferase (Biomol) (20 μ g/ml) was incubated with LipofectAMINE (100 μ g/ml) (Invitrogen) in DMEM at 22 °C for 1 h. After that the complex was diluted 10 times in DMEM and added to duplicate 18-h-old cell monolayers (~80% confluent) in serum-free medium. After 2 h the medium was removed, cells were allowed to recover for ~30 min in serum-containing DMEM, and then were seeded in 0.79-cm²-wells of chamber slides (45 \times 10³ cells/well).

Quantification of Anoikis and Measurement of Cell Viability—For fluorochrome labeling of DNA strand breaks, 6 \times 10⁵ cells were seeded in duplicate in 9.6-cm²-wells pre-coated with FN or tTG-FN in the presence or absence of RGD peptide. After 15 h incubation at 37 °C in a 5% CO₂ atmosphere, all cells (adhered and non-adhered) were collected, washed twice in PBS, resuspended at the final concentration of 1.2 \times 10⁷ cells/ml, and fixed in suspension by addition of one volume of

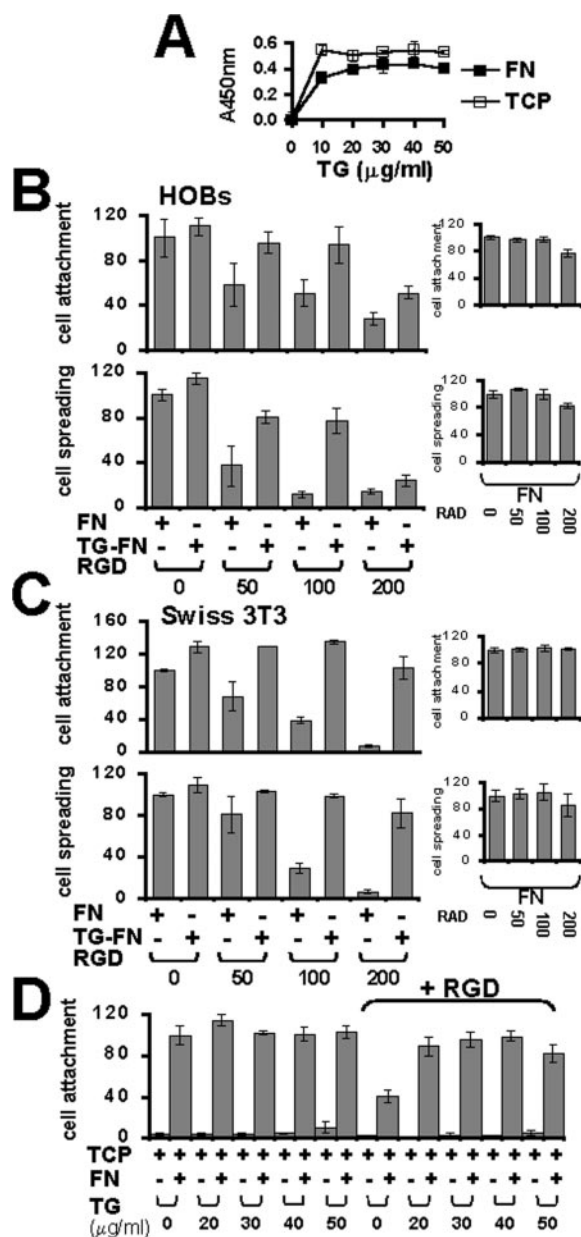


FIG. 1. tTG bound to FN but not tissue culture plastic supports RGD-independent cell adhesion. A, relative levels of tTG bound to coated FN at increasing concentrations of free tTG. Data are expressed as mean \pm S.D. absorbance at 450 nm and represent one typical experiment undertaken in triplicate. Background absorbance (in the range of 0.02–0.15) was subtracted from data. The level of tTG bound to fibronectin (FN) after incubation with 20 $\mu\text{g/ml}$ free tTG is significantly different from the level after incubation with 10 $\mu\text{g/ml}$, but not 30–50 $\mu\text{g/ml}$ tTG. The level of tTG bound to tissue culture plastic (TCP) represents the positive experimental control. B, RGD-independent cell adhesion of HOB cells and Swiss 3T3 fibroblasts (C) in response to tTG-FN. Cell attachment (upper graphs in B and C) and cell spreading (lower graphs in B and C) on FN and tTG-FN were assessed 20 min after seeding cells pre-incubated with increasing concentrations of RGD synthetic peptide (0–200 $\mu\text{g/ml}$) (RGD 0–200), as described under “Experimental Procedures.” Insets in B and C show cell attachment (upper insets) and spreading (lower insets) on FN when cells were pre-incubated with equivalent concentrations of control RAD peptide (RAD 0–200). Each point represents the mean number of attached cells (cell attachment) or the mean percentage of spread cells (cell spreading) \pm S.D. Data are expressed as percentage of control values on FN, which represents 100% and represent one of at least 3 separate experiments performed in triplicate. Mean attachment values \pm S.D. on FN control were 306 ± 53 (HOB) and 166 ± 3 (Swiss 3T3) in upper graphs, 246 ± 13 (HOB) and 155 ± 14 (Swiss 3T3) in upper insets; mean percentage values of spread cells on FN control were 78 ± 5 (HOB) and 88 ± 1 (Swiss 3T3) in lower graphs and 82 ± 2 (HOB) and 86 ± 3 (Swiss 3T3) in lower insets; total cells analyzed in control sample were ~ 900 (HOB)

4% (w/v) paraformaldehyde in PBS. Cells were then permeabilized in 0.1% (v/v) Triton X-100 in 0.1% (w/v) sodium citrate buffer for 2 min on ice (to minimize loss of fragmented DNA). Cells were labeled with terminal deoxynucleotidyl transferase (TdT) and FITC-dUTP, using a TUNEL kit according to the manufacturer's instructions (Roche). The fluorescence intensity was measured by flow cytometry using a Beckman Coulter EPICS XL. Cells were collected and data stored and analyzed using the software SYSTEM II and WinMDI2.8. DNA fragmentation was also detected by *in situ* analysis of nuclei following TUNEL, by confocal fluorescent microscopy. Cells found in suspension were fixed and labeled in triplicate on 0.79-cm²-wells of glass slides ($\sim 5 \times 10^4$ cells/well). For quantification, the Leica confocal software was used to acquire 3 random images per well for a total of 9 images per experimental sample using a fixed protocol (with constant photo-multiplier tube and section-depth setting). Data are expressed as mean number of apoptotic cells per well. Cell viability was assessed by a colorimetric assay based on the metabolism of the tetrazolium salt XTT (Roche), after an incubation period of 4 h with XTT. Data are expressed as absorbance values at 492 nm after subtraction of values at 690 nm.

Statistics—Data are expressed as mean \pm S.D. and represent one of at least 3 separate experiments undertaken in triplicate, unless stated otherwise. Differences between data sets were determined by the Student's *t* test (two-tailed distribution, two-sample equal variance). Differences described as significant in the text correspond to $p < 0.05$.

RESULTS

Tissue Transglutaminase Bound to FN Supports RGD-independent Cell Adhesion of Different Cell Types—Previous work using fluorescent microscopy and immunogold electron microscopy demonstrated a close association of tTG with FN at the cell surface/pericellular matrix (20, 22), consistent with the *in vitro*-specific binding of the enzyme with human plasma FN (13, 24). To investigate how tTG in complex with FN affects FN cell adhesion, we first bound purified guinea pig liver tTG to human plasma FN coated onto tissue culture plastic (TCP). EDTA was included in the reaction to inhibit tTG transamidating activity. Measurement of binding by an ELISA-type assay showed that FN, immobilized at the saturating concentration of 5 $\mu\text{g/ml}$, bound a saturating amount of tTG when incubated with 20 $\mu\text{g/ml}$ free tTG (Fig. 1A). Using this initial matrix model of immobilized FN with bound tTG (tTG-FN), the contribution tTG to FN cell adhesion was examined by inhibiting integrin-mediated RGD-dependent cell adhesion with competitive concentrations of soluble RGD peptides. HOBs were selected as the initial cell model because they preferentially adhere on FN *in vitro*, demonstrate an enhanced spread morphology on biomaterials coated with tTG-FN (33), and are characterized by a well defined pattern of integrin cell-surface receptors, consisting mainly of RGD-binding β_1 subunit paired with α_1 , α_2 , α_3 , α_5 , and α_V subunits (34). In the absence of RGD peptide, attachment to tTG-FN was comparable with FN (Fig. 1B, upper panel), although cell spreading appeared to be enhanced on tTG-FN (Fig. 1B, lower panel). At 50 and 100 $\mu\text{g/ml}$ RGD peptide, attachment on FN was significantly reduced (typically to 30–50% of control values on FN) (Fig. 1B, upper panel), but attachment to tTG-FN was not significantly inhibited at these same RGD peptide concentrations. Cell attachment to tTG-FN in the presence of 100 $\mu\text{g/ml}$ RGD peptide was 85–95% of control cell attachment to FN without RGD peptide. Only at 200 $\mu\text{g/ml}$ was cell attachment to tTG-FN significantly lower in comparison to control FN without RGD peptide. At

and ~ 500 (Swiss 3T3). D, comparison of HOB cell attachment to TCP with increasing concentrations of bound tTG (20–50 $\mu\text{g/ml}$) and TCP with bound FN (5 $\mu\text{g/ml}$) in complex with tTG (20–50 $\mu\text{g/ml}$). Cell attachment was assessed and expressed as described above (RGD peptide was 100 $\mu\text{g/ml}$). Mean attachment values \pm S.D. on FN control were 214 ± 22 . Total cells analyzed in control sample were ~ 700 . RGD-independent cell attachment to TCP with bound tTG did not significantly differ from cell attachment to TCP at any tTG concentration.

this higher concentration, the RGD peptide may in part act nonspecifically, because the control RAD peptide also led to a small reduction in cell attachment at 200 $\mu\text{g/ml}$ (Fig. 1B, upper inset). Incubation of cells with RGD peptide significantly reduced cell spreading on FN (Fig. 1B, lower panel), typically to 10–50% of control value at 100 $\mu\text{g/ml}$ RGD peptide, but as for cell attachment, cell spreading was only partially reduced on tTG-FN at 50 and 100 $\mu\text{g/ml}$ RGD peptide (usually to 65–85% of control values on FN). Swiss 3T3 fibroblasts displayed a comparable response to HOB cells on the tTG-FN complex. Attachment (Fig. 1C, upper panel) and spreading (Fig. 1C, lower panel) of Swiss 3T3 fibroblasts to FN was significantly decreased with excess RGD peptide, in a more sensitive way than in osteoblasts (typically to 25–35% of control at 100 $\mu\text{g/ml}$ RGD peptide), but was restored to control levels when cells were seeded onto tTG-FN at 50 and 100 $\mu\text{g/ml}$ RGD peptide. An epithelial-like cell line (ECV304) also adhered more efficiently on tTG-FN than FN in the presence of excess RGD peptide (Fig. Suppl. 1). When cells were seeded onto TCP coated with tTG without prior immobilization of FN, cell attachment was found to be negligible at concentrations ranging from 20 to 50 $\mu\text{g/ml}$ of tTG, in the absence or presence of competitive RGD peptide (Fig. 1C). Plates were coated with saturating amounts of FN, and blocking of FN-coated wells with 3% nonfat milk protein prior to tTG immobilization did not affect RGD-independent cell attachment and spreading supported by the tTG-FN matrix formed in the absence of blocking (data not shown). These findings clearly indicate that the complex of tTG bound to FN is the essential component for the RGD-independent cell adhesion to occur. Association of purified tTG to free human plasma FN in solution prior to immobilization onto TCP, with the suggested stoichiometry of $\sim 2:1$ (24), also led to a matrix able to significantly support RGD-independent cell adhesion and spreading (which respectively were 80 ± 1.4 and 98 ± 3.9 of control FN, in a typical experiment with 100 $\mu\text{g/ml}$ RGD peptide). Cells pre-treated with cycloheximide, to rule out secretion of endogenous adhesion molecules, were still capable of RGD-independent cell attachment on tTG-FN (data not shown). Together these data show that binding of tTG to FN supports a novel RGD-independent pathway.

tTG Immobilization on Amino-terminal FN Fragments Is Not Sufficient to Mediate RGD-independent Adhesion of Osteoblast-like Cells—Because tTG is known to bind to FN at a domain within the 70 kDa amino-terminal fragment (13, 24) we explored whether association of tTG to N-terminal FN peptides was sufficient to support RGD-independent cell adhesion. tTG was immobilized on the 70 kDa (matrix assembly, heparin and gelatin binding), 45 kDa (gelatin binding) and 30 kDa (first type I repeats, matrix assembly, heparin binding) amino-terminal FN peptides. Detection of the relative levels of tTG by ELISA showed that incubation of the FN fragments with 20 $\mu\text{g/ml}$ tTG resulted in saturating levels of tTG immobilized on all fragments (Fig. 2A). Cell adhesion of HOB cells to the different FN fragments alone or in complex with tTG was compared. On the 70 kDa fragment alone, both cell attachment and spreading in the absence of RGD peptide were $\sim 80\%$ the values obtained on FN (Fig. 2B, upper and lower panels, respectively); however, on the 45 kDa and 30 kDa fragments cell attachment and cell spreading were only ~ 10 and $\sim 5\%$ of control FN, respectively. In the presence of RGD peptide, cell attachment and spreading values on the 70 kDa fragment were significantly inhibited by $\sim 40\%$ (Fig. 2B, upper and lower panels, respectively). This data agrees with previous findings that the amino-terminal of FN binds the integrin $\alpha_5\beta_1$ in cross-competition with the RGD peptide (12). Immobilization of tTG on the 70 kDa fragment unlike FN did not induce RGD-inde-

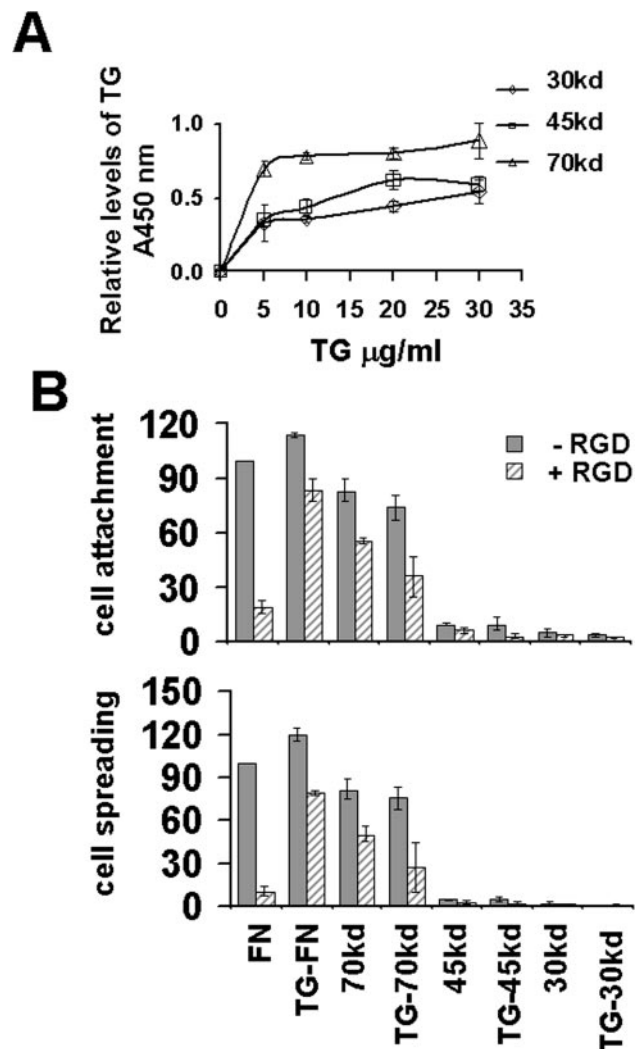
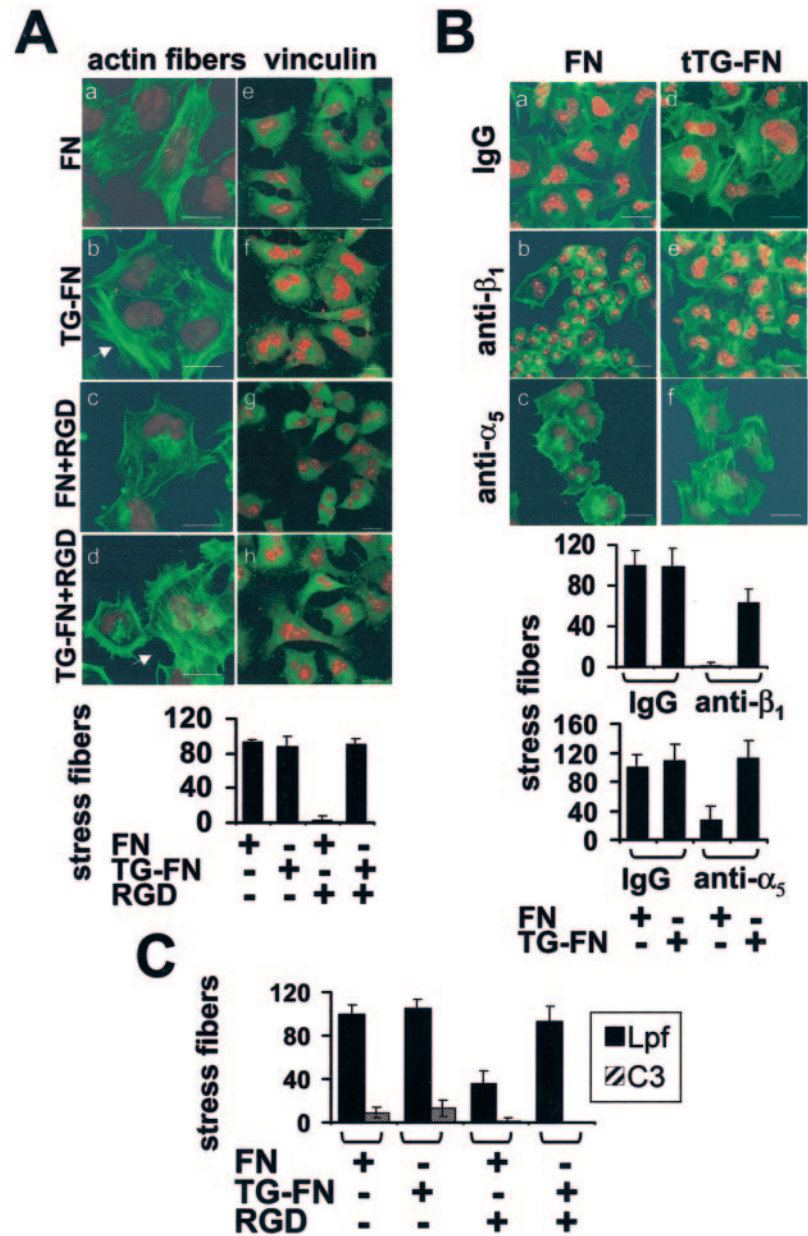


FIG. 2. tTG immobilization on amino-terminal FN fragments is not sufficient to mediate RGD-independent cell adhesion. A, relative levels of tTG bound to the amino-terminal FN fragments (70, 45, and 30 kDa) immobilized on TCP, at increasing concentrations of free tTG. Data are expressed as mean \pm S.D. absorbance at 450 nm and are from a typical experiment performed in triplicate. The level of tTG bound to each fragment after incubation with 20 $\mu\text{g/ml}$ tTG was not significantly different from the level bound using 30 $\mu\text{g/ml}$. B, assessment of cell adhesion in response to tTG bound to amino-terminal FN fragments. Wells were pre-coated with amino-terminal FN fragments, and in half of the wells 20 $\mu\text{g/ml}$ tTG was immobilized upon them (TG-70, TG-45, and TG-30). Cell attachment (B, upper panel) and cell spreading (B, lower panel) of HOB cells pre-incubated with RGD peptide (100 $\mu\text{g/ml}$) (+RGD) or DMEM (–RGD) were assessed and data expressed as described in legend to Fig. 1. In B, upper panel, ordinate represents mean cell attachment expressed as mean percentage of control attachment to FN (which represents 100%) \pm S.D. of 3 independent experiments undertaken in triplicate (mean attachment value \pm S.D. on FN in the 3 experiments was 406 ± 72 , 370 ± 49 , and 465 ± 51 ; total cells analyzed in control samples were respectively ~ 1200 , ~ 1100 , and ~ 1400). In B, lower panel, ordinate represents the mean percentage of spread cells, expressed as mean percentage of control spreading on FN \pm S.D. of 3 independent experiments undertaken in triplicate (mean percentage of spreading \pm S.D. on FN in the 3 experiment was 87 ± 1 , 91 ± 1 , and 88 ± 7).

pendent cell attachment and spreading but led to further deterioration of cell adhesion (Fig. 2B). Yet tTG did not enhance cell adhesion to the 70-kDa fragment even in the absence of the RGD peptide. Furthermore, tTG did not improve cell adhesion on the 45-kDa and 30-kDa fragments, which remained at negligible levels (Fig. 2B). These results indicate that adhesion of HOB cells to the amino-terminal 45 kDa and 30 kDa FN fragments, which contain putative tTG-binding sites (13, 24), is

FIG. 3. Confocal laser fluorescence microscopy of RGD-independent actin cytoskeleton organization and focal adhesion in response to tTG-FN. A, visualization of actin stress fibers and focal adhesions in the presence of RGD peptide. Cells were seeded as in legend to Fig. 1 and the indicated cells pre-treated with RGD peptide (100 $\mu\text{g}/\text{ml}$) (RGD). Actin stress fibers and focal adhesions were revealed as described under “Experimental Procedures.” Images were acquired by confocal laser fluorescence microscopy, and cells in random fields (at least 100 cells in FN control) were scored for actin stress fiber formation as outlined under “Experimental Procedures.” Data shown in the histogram are from a representative experiment. Ordinate represents the mean percentage of cells with formed actin stress fibers expressed as percentage of control values on FN. Mean \pm S.D. percentage of cells with stress fibers formed on control FN was 74 ± 2 . Arrows point to tTG-FN-mediated stress fibers with and without RGD peptide. Bars = 10 μm . B, actin stress fibers in the presence of function blocking anti-integrin α_5 and β_1 antibodies. HOB cells in suspension were pre-incubated with anti-integrin antibodies P1D6 (α_5) and JB1A (β_1) or control mouse IgGs (IgG) before seeding on either FN or tTG-FN as described in A. At least 200 cells in FN/IgG control were scored. Mean percentage value of cells with actin fibers formed on control FN \pm S.D. was 49 ± 8.4 in B, upper panel, and 53 ± 7.8 in B, lower graph. Bars = 10 μm . C, relative measurement of actin stress fibers following pre-incubation with the RhoA inhibitor C3 exotransferase. Monolayers of HOB cells were loaded with C3 exotransferase (C3), or Lipofectin only (Lpf), as described under “Experimental Procedures” and then seeded as described in A. At least 250 cells in FN/Lpf control were scored. Mean percentage value of cells with actin fibers formed on control FN \pm S.D. was 63 ± 5 .



negligible regardless of the binding of tTG, and that tTG binding to the 70-kDa peptide is not sufficient to sustain RGD-independent cell adhesion.

RGD-independent Cell Adhesion to FN with Immobilized tTG Promotes Formation of Unique Focal Adhesion Structures—Formation of actin stress fibers in the presence of integrin-binding RGD peptide in response to tTG-FN was analyzed by confocal laser scanning microscopy utilizing FITC-phalloidin. HOB cells adhered to FN did not show organized stress fibers following RGD peptide treatment (Fig. 3A, panel c), compared with non-treated cells (Fig. 3A, panel a), which exhibited a flat morphology and extensive actin stress fibers. In contrast, most of the cells seeded on tTG-FN were spread and had organized actin stress fibers despite the RGD peptide (Fig. 3A, panel d); however, the actin fibers formed were shorter and less organized than those assembled in control cells adhered to FN in the absence of RGD peptide (Fig. 3A, panel a). Without RGD peptide, actin stress fibers appeared more dense and well formed in response to tTG-FN than FN (Fig. 3A, panels b and a, respectively), confirming that immobilized tTG enhances cell spreading (see Fig. 1B). Staining for vinculin indicated the

absence of punctate characteristic focal contacts of FN-adhered cells (Fig. 3A, panel e) in the RGD-treated cells adhered to FN (Fig. 3A, panel g) but not in those adhered to tTG-FN (Fig. 3A, panel h). Relative measurement of the formed actin stress fibers (Fig. 3A, graph) confirmed that the RGD peptide did not affect the formation of focal adhesions in cells plated on tTG-FN, although it significantly affected the quality of the actin reorganization, as shown by fluorescence microscopy (Fig. 3A, panel d). Treatment of cells with the function blocking anti-integrin β_1 (JB1A) and, to a lesser extent, α_5 antibody (PID6), led to a large decrease of actin stress fibers on FN (Fig. 3B, panels b and c, respectively), compared with cells incubated with nonspecific IgG (Fig. 3B, panel a). In contrast, on tTG-FN, cells incubated with the anti-integrin antibodies appeared to maintain a network of actin stress fibers (Fig. 3B, panels e and f), although less elaborated and dense than in control cells treated with IgGs (Fig. 3B, panel d). Comparison of the number of formed actin stress fibers (Fig. 3B, graph) statistically confirmed these observations that tTG-FN leads to the formation of integrin β_1 - and α_5 -independent actin filaments even though more rudimental than in the absence of inhibition. RGD-inde-

pendent adhesion of cells to tTG-FN was dependent on GTPase RhoA, because inhibition of RhoA activity by botulinum toxin C3 exotransferase almost completely blocked RGD-independent assembly of actin stress fibers in response to tTG-FN (Fig. 3C).

tTG Cross-linking Activity Is Not Required to Support RGD-independent Cell Adhesion—We next assayed the transamidating activity of FN-bound tTG to establish its potential role in the described RGD-independent cell adhesion process. The activity of tTG once bound to FN was negligible when measured in cell culture medium DMEM, which contains an activating concentration of Ca^{2+} (1.9 mM), and was not changed by addition of further Ca^{2+} , but was significantly boosted by pre-incubation of tTG with DTT prior to immobilization on FN (Fig. 4A), as described previously (26). Hence, under the conditions used FN-bound tTG is not active in the presence of cell culture medium, unless its cysteine residues, particularly the active-site Cys²⁷⁷, are kept in a reduced state. The transamidation-independent role of tTG in the RGD-independent cell adhesion process was further confirmed by utilizing the irreversible inhibitor R283, a 2-[(2-oxopropyl)thio]imidazolium derivative (19). HOB cells were incubated with R283 and plated on a tTG-FN matrix pre-treated with R283, in the absence or presence of RGD peptide. Under these conditions the activity of the immobilized tTG is completely blocked by the inhibitor (Fig. 4C). The low tTG activity found at the HOB cell surface (30) is also inhibited to negligible values by equal concentrations of R283.² Cell adhesion on FN bound to inactivated tTG was not significantly different from cell adhesion on FN bound to tTG not treated with the inhibitor, with or without pre-treatment of cells with RGD peptide, and it was typically twice cell adhesion on FN in the presence of RGD peptide (Fig. 4B, cell attachment, upper panel; cell spreading, lower panel). These data clearly indicate that FN-bound tTG does not require its transamidating activity to promote RGD-independent cell adhesion.

Evidence for the Importance of FN-associated tTG and its Calcium-induced Conformation in Cell-surface Recognition—To assess the importance of tTG in cell-surface interaction, FN-bound tTG was blocked by using the monoclonal anti-tTG antibody Cub74 in conditions that fully preserved the availability of FN in this complex. This was demonstrated by the unchanged recognition of FN by anti-FN polyclonal antibody after treatment of tTG-FN with either Cub74 or control IgG (Fig. 5B). Obstruction of tTG by Cub74 completely abolished the RGD-independent cell adhesion mediated by tTG-FN (Fig. 5A, cell attachment, upper panel; cell spreading, lower panel), suggesting a direct role for FN-associated tTG in the RGD-independent binding to cells. tTG can assume two conformations, depending on whether it is bound to GTP/GDP or Ca^{2+} (18). In the extracellular environment, tTG is likely to assume the Ca^{2+} -induced open structure. Incubation of FN-bound tTG with the non-hydrolysable GTP- γ S (1 mM) significantly reduced the RGD-independent cell attachment and spreading mediated by tTG-FN (Fig. 5C, upper and lower panels, respectively). Because incubation of tTG with GTP- γ S did not significantly alter the level of tTG bound to FN (Fig. 5D), our results suggest that RGD-independent cell adhesion to tTG-FN critically depends on the calcium-mediated tertiary structure of tTG.

Role of Cell-surface Heparan Sulfate in RGD-independent Cell Adhesion and Signaling via tTG-FN—To explore the possibility that cell adhesion to tTG-FN may be mediated by a cell-surface proteoglycan, HOB cells were treated with glycosaminoglycan-degrading enzymes. Degradation of cell-surface

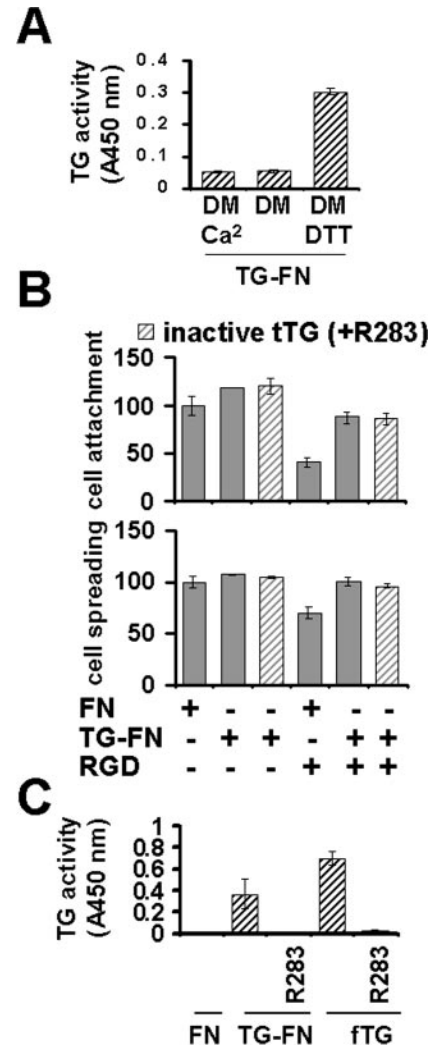


FIG. 4. tTG cross-linking activity is not required to support RGD-independent cell adhesion to tTG-FN. A, the activity of FN-bound tTG (TG-FN) was measured by incorporation of biotinylated cadaverine into FN in either culture medium DMEM (DM), or DMEM with 5 mM Ca^{2+} (DM- Ca^{2+}), or DMEM supplemented with 5 mM DTT (DM-DTT). Values represent the mean \pm S.D. absorbance at 450 nm of one typical experiment undertaken in triplicate. B, cell adhesion to tTG-FN following inactivation of tTG. The tTG-FN matrix was incubated with the tTG irreversible inhibitor R283 (100 μ M) and then utilized as adhesive substrate for HOB cells, further supplemented with the same concentration of R283. In controls, identically treated cells were seeded on tTG-FN without R283 treatment. Where indicated, cells were pre-incubated with RGD peptide (100 μ g/ml). Cells were examined for cell attachment (B, upper panel) and cell spreading (B, lower panel) and data expressed as percentage of control values on FN as in the legend to Fig. 1. Mean attachment value on FN control \pm S.D., 373 ± 36 in B, upper panel; mean percentage value of spread cells \pm S.D. on FN control, 89 ± 6 in B, lower panel; total cells analyzed in control sample, ~ 1100 . Data shown are from a representative experiment undertaken in triplicate. C, inhibition of the cross-linking activity of FN-bound tTG (TG-FN) and tTG-free in solution (tTG) by 100 μ M R283, when measured as described in A, in buffer containing DTT. Values represent the mean \pm S.D. of a representative experiment undertaken in triplicate.

heparan sulfate chains with heparitinase (15 milliunits/ml) led to a reduced cell attachment to FN ($\sim 70\%$ of control values) (Fig. 6A, upper panel), as expected given the importance of cell-membrane HSPG in the adhesion of osteoblast-like cells (34). It also led to complete abolishment of RGD-independent cell attachment and spreading on tTG-FN (Fig. 6A, upper and lower panels, respectively). In contrast, equal concentrations of protease-free chondroitinase ABC had no significant effect on cell adhesion to FN, did not significantly alter RGD-independ-

² D. Telci, E. A. M. Verderio, and M. Griffin, unpublished data.

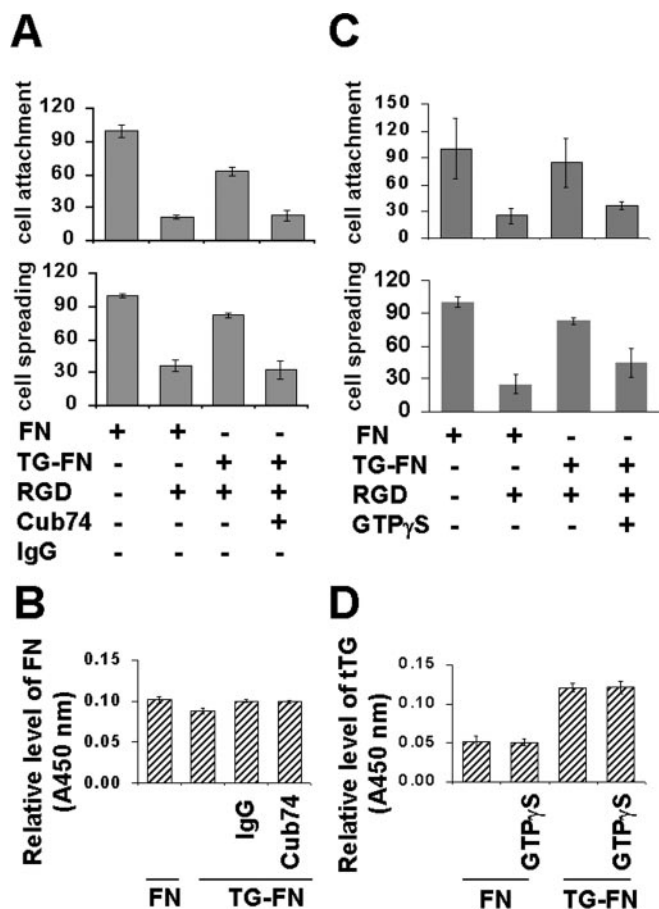


FIG. 5. RGD-independent cell adhesion to FN-bound tTG depends on tTG accessibility and GTP-mediated conformational change. *A*, FN-bound tTG was blocked by incubation with Cub74 (40 μ g/ml) for 1 h at 37 $^{\circ}$ C in PBS with 2 mM EDTA using mouse IgG1k as control antibody. Following pre-incubation with RGD peptide, cells were seeded on the tTG-FN matrix. Adhered cells were examined for cell attachment (*A*, upper panel) and cell spreading (*A*, lower panel) and data expressed as in the legend to Fig. 1. Mean attachment value \pm S.D. on FN control, 229 ± 13 in *A*, upper panel; mean percentage value of spread cells \pm S.D. on FN control, 93 ± 2 in *A*, lower panel; total cells analyzed in control sample, ~ 700 . Data are from a typical experiment undertaken in triplicate. *B*, availability of FN, detected as described under "Experimental Procedures," after blocking the tTG-FN matrix by Cub74 and IgG1k. Values represent the mean \pm S.D. absorbance at 450 nm of 4 replicates from a typical experiment. *C*, HOB cells in suspension, pre-incubated with RGD peptide (100 μ g/ml) as indicated, were seeded in the presence of 1 mM GTP- γ S on FN-bound tTG, pre-incubated with 1 mM GTP- γ S in PBS for 10 min at room temperature. Adhered cells were examined for cell attachment (*C*, upper panel) and cell spreading (*C*, lower panel) with and without inactivation of tTG by GTP- γ S and data expressed as in the legend to Fig. 1. Mean attachment value \pm S.D. on FN control, 294 ± 98.32 in *C*, upper panel; mean percentage value of spread cells \pm S.D. on FN control, 84.9 ± 4 in *C*, lower panel; total cells analyzed in control sample, ~ 800 . Data are from a typical experiment undertaken in triplicate. *D*, relative levels of tTG that bind FN in the presence of 1 mM GTP- γ S, in conditions identical to *C* above. tTG was detected by an ELISA-type assay described in the "Experimental Procedures." Values represent the mean \pm S.D. absorbance at 450 nm of 4 replicates from a representative experiment.

ent cell spreading on tTG-FN (Fig. 6A, lower panel), and only marginally affected cell attachment (Fig. 6A, upper panel). These results demonstrate that RGD-independent cell adhesion to tTG-FN critically depends on cell-surface heparan sulfate and suggest the involvement of cell-surface HSPG and not chondroitin sulfate proteoglycans in this process. Syndecan-4 is the only known HSPG that is a widespread component of focal adhesions, and downstream signaling specifically involves PKC α (35). Cells were therefore treated with the selective PKC α inhibitor G06976 (36) prior to and during the cell adhe-

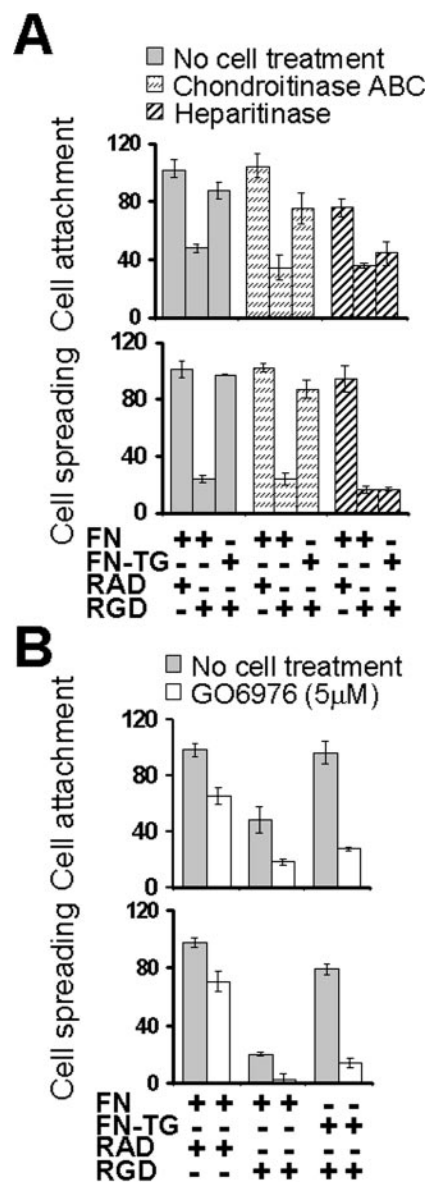


FIG. 6. RGD-independent cell adhesion to tTG-FN is dependent on cell surface heparan sulfate and PKC α activity. *A*, HOB cells in suspension (2×10^5 cell/ml) were pre-treated with 15 milliunits/ml heparitinase or 15 milliunits/ml protease-free chondroitinase ABC in serum-free medium for 1 h at 37 $^{\circ}$ C before evaluating cell attachment (upper panel) and cell spreading (lower panel) in the presence of RGD or RAD peptide (100 μ g/ml). Data are produced and expressed as in the legend to Fig. 1 and represent percentage of control values on FN from one of 3 separate experiments. Mean attachment values \pm S.D. on FN control without peptide treatment (not shown), 140 ± 16 ; mean percentage values of spread cells on FN control, 89 ± 2 ; total cells analyzed in control sample, ~ 420 . *B*, monolayers of sub-confluent HOB cells were serum-starved for 12 h and then incubated in serum-free DMEM medium supplemented with the PKC α inhibitor G06976 (5 μ M, dissolved in Me $_2$ SO) for 1 h or with an equal volume of Me $_2$ SO only. Cells were then harvested and analyzed for cell attachment (upper panel) and spreading (lower panel) on FN and tTG-FN. Data, expressed as percentage of control values on FN, are from one of 3 separate experiments. Mean attachment and spread cell values \pm S.D. on FN control without peptide (not shown), 197 ± 8 and 83 ± 4 , respectively; total cells analyzed in control sample, ~ 590 .

sion experiments. Following G06976 incubation, a significant inhibition ($\sim 30\%$) of both attachment and spreading on FN (Fig. 6B, upper and lower panels, respectively) with control RAD and RGD peptide occurred, which was comparable with the inhibition of attachment following heparitinase (Fig. 6A, upper panel). However, the PKC α inhibitor drastically reduced

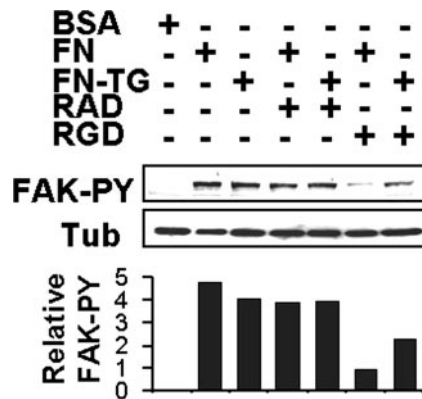


FIG. 7. RGD-independent adhesion to tTG-FN promotes tyrosine phosphorylation of FAK. Lysates of HOB cells grown in the presence of RGD or RAD control peptide (100 $\mu\text{g/ml}$) on FN, tTG-FN, or control bovine serum albumin-coated TCP, were Western blotted and then immunoprobed with Tyr(p)³⁹⁷-FAK antibody followed by peroxidase conjugate anti-rabbit IgG (FAK-PY), as described under “Experimental Procedures.” After stripping, blots were re-probed to reveal control protein tubulin (*Tub*). Density of bands was quantified by scanning densitometry, and phospho-FAK bands normalized against values for tubulin bands (*relative FAK-PY*). Results from one of three typical experiments are shown.

RGD-independent attachment (over 90%) and spreading (~85%) mediated by the tTG-FN complex (Fig. 6B), indicating that cell adhesion mediated by tTG-FN critically depends on PKC α activity. This finding also hints at syndecan-4 as the likely HSPG responsible for binding the tTG-FN complex.

RGD-independent Adhesion in Response to tTG-FN Enhances Tyrosine Phosphorylation of FAK—Having shown that tTG-FN transmits signals via a heparan sulfate receptor leading to cell spreading and that this process depends on the activity of PKC α , we next examined whether the attachment to tTG-FN led to activation of FAK. Tyrosine phosphorylation of FAK in cells plated on FN and treated with RGD peptide was decreased to ~25% of that found in control cells plated on FN and pre-incubated with control RAD peptide (Fig. 7). In response to tTG-FN instead, the level of FAK phosphorylation in the presence of RGD peptide was found to be ~60% of the level of both control cells on FN or tTG-FN. This data shows that the RGD-independent cell adhesion mediated by tTG-FN enhances tyrosine phosphorylation of FAK and as such implies FAK as one of the intracellular signaling mediators of tTG-FN.

RGD-independent Cell Adhesion Can be Mediated by a Physiological Matrix of Cell-assembled FN and Cell-secreted tTG—We have previously shown (19, 20, 22, 37) that increased expression of tTG within cells results in an increased export of the enzyme into the extracellular matrix. Such a phenomenon has been observed during cell stress and following cell wounding (16, 17). To produce such a cell model, conditioned matrices of cell-assembled FN with different bound levels of cell-secreted tTG were obtained from a long-term culture of a transfected fibroblast cell line (Swiss 3T3-TG3), capable of tetracycline (tet) regulatable expression of tTG (22). Cells were then removed from both conditioned matrices, and in their place wild-type Swiss 3T3 fibroblasts were seeded and allowed to adhere in the presence of increasing concentrations of RGD peptide. The FN-rich ECM with increased amounts of cell-secreted tTG (ECM/TG3-tet) (Fig. 8B) supported significantly higher RGD-independent cell attachment at each RGD peptide concentration, compared with the ECM with background levels of tTG (ECM/TG3+tet) (Fig. 8A). RGD-independent cell attachment on the lower tTG containing ECM/TG3+tet could be significantly increased by immobilization of purified tTG on this matrix (ECM/TG3+tet plus tTG) (Fig. 8A). However, at low

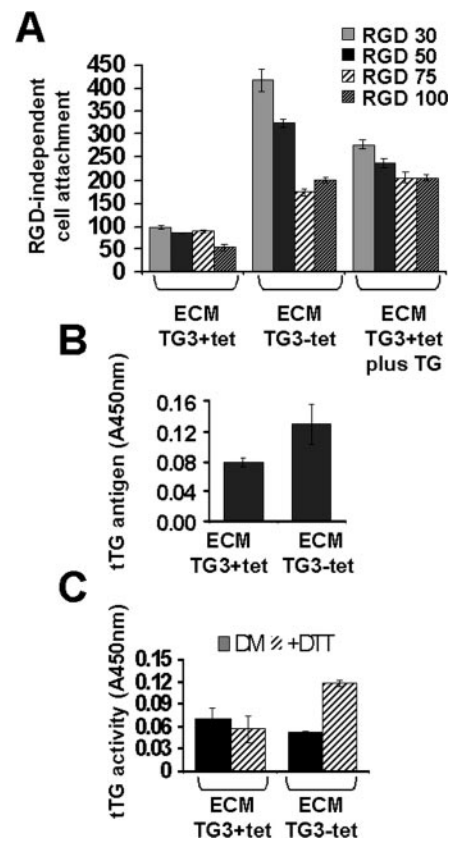


FIG. 8. A physiological matrix of FN and cell-secreted tTG supports RGD-independent cell adhesion of Swiss 3T3 fibroblasts. **A**, Swiss 3T3-TG3 cells were grown on TCP either in the absence of tet, to induce the expression of tTG and deposit an ECM rich in tTG (ECM/TG3-tet), or in the presence of tet, to inhibit tTG overexpression and deposit a ECM with background levels of tTG (ECM/TG3+tet). Cells were then removed by 5 mM EDTA in PBS, and the remaining matrices used to measure the attachment of wild-type Swiss 3T3 fibroblasts, pre-incubated with increasing concentrations of RGD peptide (30–100 $\mu\text{g/ml}$). RGD-independent adhesion was also tested on ECM/TG3+tet supplemented with purified tTG (20 $\mu\text{g/ml}$), which was immobilized as done on purified FN (ECM/TG3+tet plus TG). Each point represents the mean number of attached cells \pm S.D. of a representative experiment performed in triplicate. **B**, relative levels of tTG in the ECM of cells overexpressing tTG (TG3-tet) and with background tTG (TG3+tet). tTG was detected by an ELISA-type assay described under “Experimental Procedures.” Values represent the mean \pm S.D. of 6 replicates from a representative experiment. **C**, cross-linking activity of tTG in ECM/TG3+tet and ECM/TG3-tet, measured by the incorporation of biotinylated cadaverine into FN in culture medium DMEM in the absence (DM) or presence of 5 mM DTT (DTT). Data represent the mean \pm S.D. of 3 replicates from a typical experiment.

levels of RGD peptide, cell attachment was still more effective on the ECM containing cell-secreted tTG (ECM/TG3-tet) than on the ECM containing added tTG (ECM/tTG3+tet plus tTG). This was despite higher levels of tTG present following exogenous addition of TG (data not shown), suggesting that cell-secreted tTG is better presented to the cell surface. The ECM deposited by cells with increased levels of tTG (ECM/TG3-tet) showed no significant difference in tTG enzymatic activity above background (ECM/TG3+tet) in culture medium, unless in the presence of reducing agent (Fig. 8C). This is consistent with the idea that tTG activity is gradually down-regulated once sequestered in the oxidizing extracellular environment.

FN-bound tTG Rescues Primary Dermal Fibroblasts from Anoikis—A potential physiological function of the tTG-mediated RGD-independent cell adhesion is the protection from apoptosis (anoikis) triggered by inhibition of RGD-dependent adhesion. This phenomenon could occur in tissue injury when changes in the ECM composition lead to reduction of RGD-de-

pendent cell adhesion (5, 8), and the increased externalization and binding of tTG to the FN matrix in response to wounding (16, 17) may result in an alternative adhesion-dependent survival pathway. Non-confluent cultures of mouse dermal fibroblasts devoid of tTG (MDF-TG^{-/-}) were plated on FN or tTG-FN and incubated with RGD peptide under serum-free conditions. After ~15 h, the majority of the RGD-treated cells plated on FN were detached and displayed morphological signs of apoptosis. The extent of endonucleolysis was measured by fluorescent labeling of DNA strand breaks using TUNEL and quantified by flow cytometry (Fig. 9A). After incubation with the RGD peptide ~24% of the total fibroblasts grown on FN were apoptotic (*black histogram*) compared with only ~2.6% of fibroblasts grown on tTG-FN (*blue histogram*), which behaved similarly to control cells grown on FN in the absence of RGD peptide (*green histogram*). These data were corroborated by *in situ* fluorescent labeling of nuclei undertaken on the detached cells in suspension, which was visualized and scored by confocal microscopy (Fig. 9B). At 15 h exposure to the RGD peptide, a significantly lower number of apoptotic cells were found in the culture fluid of cells grown on tTG-FN compared with FN. The level of apoptosis upon incubation on tTG-FN was comparable with that found in the culture medium of control cells on FN without the RGD peptide (Fig. 9B). After 30 h incubation in the absence of serum, nuclear fragmentation appeared to increase not only in cells grown with RGD peptide but also in cells grown on FN without RGD peptide, thus limiting our investigations to ~15 h time-period (Fig. 9B). We next assayed the viability of MDF-TG^{-/-} in response to tTG-FN (Fig. 9C). Cell viability on FN was significantly decreased after 15-h exposure to RGD peptide, compared with control RAD peptide (Fig. 9C), in agreement with the level of total apoptotic cell death measured in the same conditions by flow cytometry (Fig. 9A). In contrast, cell viability on tTG-FN was not substantially altered by incubation with RGD peptide, and it was found to be ~30% higher than on FN (Fig. 9C), indicating that attachment to tTG-FN mediates RGD-dependent cell survival.

DISCUSSION

The impact of tTG, a well characterized FN-associating protein and modulator of the FN matrix on FN-mediated cell survival has never been investigated (38). Whereas previous studies have analyzed the roles of tTG by modulating its expression (22, 25, 26, 39), in the present study we have developed a model that allows us to characterize cellular responses to a tTG-rich FN matrix, thus mimicking physio/pathological conditions *in vivo*. Support for our model comes from findings that tTG is not only externalized under normal physiological conditions but it is also up-regulated, exported, and deposited into the ECM in response to tissue trauma following cellular damage, inflammation, or cell stress (16, 17, 40), where it either binds FN fibrils directly or plasma FN (20, 22, 24), which is then deposited in the damaged area. Hence a complex of tTG and FN, formed as a result of matrix alterations during tissue injury, may provide a mechanism to ensure adhesion-mediated cell survival in wound-repair in response to the reduction or loss of RGD-dependent cell adhesion (8, 5).

To test this hypothesis, we initially examined the function of the tTG-FN complex in cell-matrix interactions whereby we inhibited the “classical” adhesion-mediated survival pathway dependent on the interaction of the FNIII₁₀ RGD cell-binding site with $\alpha_5\beta_1$ integrins. A human osteoblast-like cell line served as the initial cell model because osteoblasts secrete both FN and tTG (30, 34, 41) are subject to continuous matrix remodeling processes during their differentiation, are characterized by a well defined and simple pattern of integrin cell surface receptors, mainly β_1 , and make use of RGD-independ-

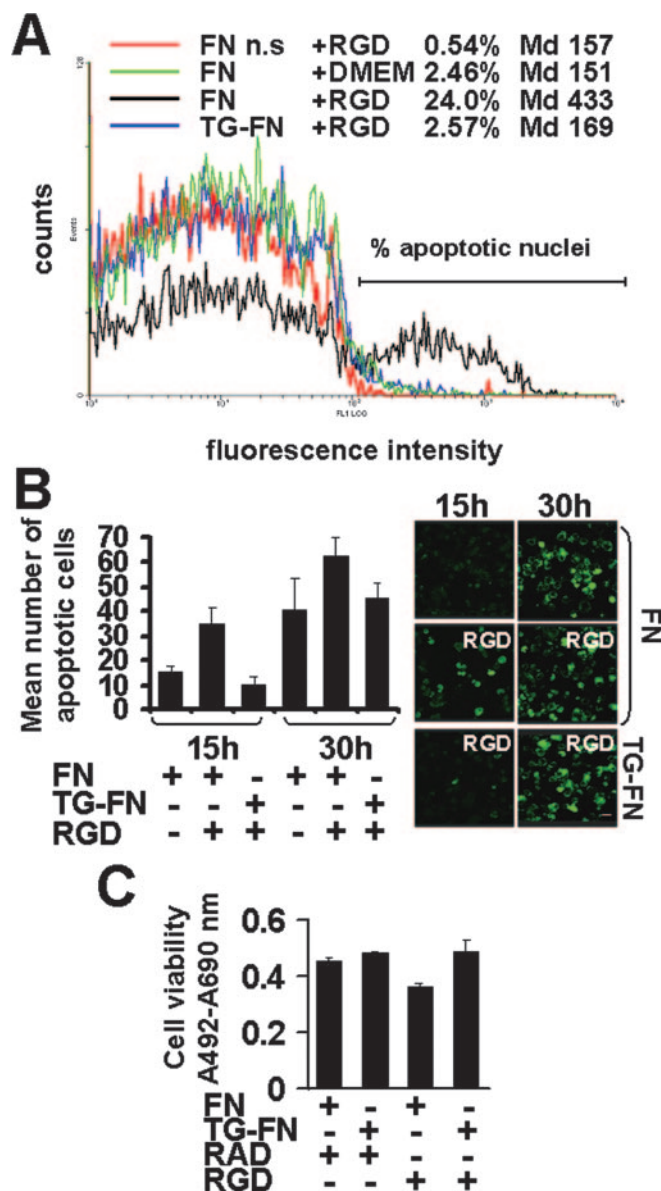


FIG. 9. Cell attachment to tTG-FN promotes cell survival of tTG-null dermal fibroblasts induced to undergo apoptosis by inhibition of RGD-dependent integrin function. **A**, flow cytometric analysis of apoptosis in tTG-null mouse dermal fibroblasts (MDF-TG^{-/-}). Cells were seeded in medium containing RGD peptide (100 μ g/ml) or DMEM only, on FN or tTG-FN for 15 h. As a measure of apoptosis, nuclear fragmentation of both adherent and detached cells was detected by TUNEL and quantified by flow cytometry as described under “Experimental Procedures.” The bar denotes the positive region of fragmented nuclei (% apoptotic nuclei), set by the negative standard (*n.s.*) of cells undergoing anoikis and incubated with FITC-dUTP in the absence of the enzyme TdT (*red histogram*). *Md*, median fluorescence channel. **B**, *In situ* analysis of nuclear fragmentation of MDF-TG^{-/-}. Cells were treated with RGD peptide and incubated as described in **A**. After 15 h and 30 h growth, the fractions of cells in suspension were processed for *in situ* detection of DNA fragmentation, which was scored by confocal fluorescent microscopy as described under “Experimental Procedures.” Data represent the mean number \pm S.D. of apoptotic cells/well from a typical experiment undertaken in triplicate. Total cells analyzed, ~450 and ~400 at 15 h and 30 h, respectively. *Bar* = 10 μ m. **C**, cell viability assay of MDF-TG^{-/-}. Cells were grown in medium containing RGD or control RAD peptide (100 μ g/ml) on FN or tTG-FN for 15 h, as described above. Cell viability was tested following incubation of cells with XTT. Data represent the mean \pm S.D. of a typical experiment performed in quadruplicate.

ent pathways in the attachment to the ECM (34). We demonstrate that the loss of cell-matrix interaction by inhibition of RGD-dependent integrin function can be largely re-established

upon seeding of cells on either FN with associated tTG or a more physiological matrix of cell-assembled FN containing cell-secreted tTG. This latter form of tTG-FN matrix is thought to be the most important form present *in vivo* as in tissues, FN is present as an insoluble fibrillar matrix to which tTG is closely associated (20, 22). Restoration of cell adhesion by tTG-FN following RGD inhibition was also found in mouse Swiss 3T3 fibroblasts and in the epithelial-like cells ECV-304, suggesting that many cell types can use the RGD-independent cell-adhesion pathway mediated by tTG-FN.

We demonstrate that cell adhesion to tTG-FN is not linked to modification of FN by calcium-dependent transamidation. This finding is consistent with recent observations indicating a transamidating-independent role for tTG in cell-matrix interactions (19, 27, 28). Moreover we show that when tTG is complexed with FN it becomes catalytically inactive unless kept in a reduced state. Indeed, previous work has described that tTG sequestration by FN leads to down-regulation of enzymatic activity on large-size protein substrates (24). In contrast, *in situ* tTG activity demonstrated with small-size fluorescent primary amine substrate has clearly shown that tTG is catalytically active while present at the cell surface (22). tTG may modify FN by its intrinsic protein disulfide isomerase (PDI) activity, which has been recently ascribed to it (42). However, because GTP binding to tTG affects the adhesion function of FN-bound tTG but does not affect the PDI activity of tTG this possibility seems unlikely.

The outside-in signaling induced by the RGD-independent cell adhesion to tTG-FN appears to result by direct interaction of tTG with the cell surface, because the blocking of tTG accessibility by a monoclonal antibody greatly reduces this process. The calcium-mediated tertiary structure of tTG is also required, suggesting that crucial cell-binding sites might be exposed when tTG assumes the calcium-induced open conformation. However, the simple binding of 20 $\mu\text{g/ml}$ tTG to either tissue culture plastic or the gelatin-binding domain of FN, which contains the tTG-binding site (13), does not enhance cell adhesion, which is indeed equally negligible regardless of the presence of tTG, in contrast to what has been previously reported (27, 28). We also found that tTG binding to the 70 kDa amino-terminal fragment of FN, which can support cell adhesion and includes the tTG-binding site, is not sufficient to sustain tTG-mediated RGD-independent cell adhesion. This leads us to conclude that the RGD-independent adhesion to tTG-FN is both tTG- and FN-dependent, with the amino-terminal of FN required to support tTG binding and the carboxy-terminal of FN and/or cryptic epitopes outside the FNIII₉₋₁₀ domains, essential to sustain the RGD-independent pathway.

Our data also suggest that the RGD-independent cell adhesion to tTG-FN is integrin-independent or, alternatively, the integrin must be in partnership with some other receptor(s). This observation is supported by the finding that tTG-mediated focal adhesions still formed in the presence of function blocking anti-integrin antibodies β_1 and α_5 , which cause conformational inactivation of the receptor, thus preventing outside in signaling (43). Under these conditions the actin stress fibers formed appeared less complex than normal, nevertheless the cytoarchitecture was sufficient for the formation of distinct RGD-independent focal adhesions, which are mediated by GTPase RhoA and induce FAK tyrosine phosphorylation. Therefore, modulation of matrix FN by tTG adds to the increasing number of non-integrin-mediated stimuli, which enhance FAK activity through actin polymerization (44). The possibility that tTG-FN may mediate RGD-independent cell adhesion through the $\alpha_4\beta_1$ -induced RGD-independent pathway is also unlikely because low or negligible levels of α_4 subunit are generally expressed in

osteoblasts (34). Moreover, matrix binding to $\alpha_4\beta_1$ does not generate actin stress fibers (45). Although tTG association with integrins is documented, our data suggest that it is more likely that the cell function induced by tTG-FN results from the binding to non-integrin receptors. Given the high affinity binding of tTG for heparin (46), a possible candidate receptor for tTG-FN is that belonging to the class of HSPG (35). Treatment of HOB cells with heparitinase but not chondroitinase ABC greatly diminished the RGD-independent adhesion in response to tTG-FN, suggesting that cell surface HSPG may mediate RGD-independent cell adhesion to tTG-FN. The C-terminal HepII domain of FN is responsible for the synergistic interaction of FN with cell surface heparan sulfate and integrins, and this interaction is essential for optimal cell adhesion and critical for sustained cell survival (7, 35). Association of tTG with FN could induce RGD-independent cell adhesion by reinforcing HSPG-mediated adhesion, through a dual mechanism involving the binding of tTG to cell surface HSPG and increased exposure of the C-terminal heparin-binding domain of FN, which critically depends on FN structure (9). The increased cell spreading observed in osteoblasts and Swiss 3T3 fibroblasts in early cell adhesion to tTG-FN also in the absence of integrin inhibition suggests that HSPG receptors are not fully occupied when cells are normally seeded on a FN matrix and that increased binding occurs in response to tTG-FN. Downstream signaling from syndecan-4, the only HSPG that is a widespread component of focal adhesion, specifically results in hyperactivation of PKC α and activation of both RhoA and FAK (7, 35). Our results suggest that RGD-independent cell adhesion mediated by tTG-FN requires PKC α activity because the compound G66976, which is the only inhibitor available that shows specificity for PKC α (36), blocks this process. Our data also show that the function of FN-bound tTG depends on RhoA activation and is linked to activation of the cell survival kinase FAK (1, 44).

Moreover, in preliminary investigations using a Raf-1-null 3T3 like immortalized fibroblast cell line (47) we could demonstrate that the RGD-independent cell adhesion pathway by tTG-FN is not functional in this cell line.³ This suggests that the Raf-1 protein, whose main function is anti-apoptotic (47), may be a key component in the signaling pathway mediated by tTG-FN. The observation that a tTG-FN matrix can rescue tTG-null primary dermal fibroblasts from anoikis with maintenance of cell viability is therefore consistent with its activation of intracellular survival mediators. Importantly, it shows that the survival role of tTG is essentially extracellular and not intracellular as recently suggested by Antonyak *et al.* (48), following up-regulation of tTG by retinoic acid.

It is now accepted that RGD-mediated cell adhesion is not sufficient in isolation to maintain cell survival. For sustained survival cells need to interact with "complex" ECMs via integrin and non-integrin receptors, such as cell surface proteoglycans (7). Interestingly like tTG, increased expression of syndecan-4 is also found at sites of tissue injury (35). The work presented here indicates that binding of tTG to FN represents one additional survival signal by inducing heparan-sulfate receptors-mediated cell adhesion, which can either act in synergy or in alternative to integrin RGD-dependent cell adhesion at sites of tissue injury.

Acknowledgments—We thank Dr. M. Baccarini (Vienna Biocenter, Vienna, Austria) for critically reading the manuscript and for donating the Raf-1-null 3T3-like immortalized fibroblasts and M. Stevenson for help with the compilation of the manuscript.

³ D. Telci, E. A. M. Verderio, M. Baccarini, and M. Griffin, unpublished data.

REFERENCES

1. Frisch, S. M., and Sreaton, R. A. (2001) *Curr. Opin. Cell Biol.* **13**, 555–562
2. Boudreau, N., Sympson, C. J., Werb, Z., and Bissell, M. J. (1995) *Science*. **267**, 891–893
3. Davis, G. E., Bayless, K. J., Davis, M. J., and Meininger, G. A. (2000) *Am. J. Pathol.* **156**, 1489–1498
4. Sechler, J. L., and Schwarzbauer, J. E. (1998) *J. Biol. Chem.* **273**, 25533–25536
5. Hadden, H. L., and Henke, C. A. (2000) *Am. J. Respir. Crit. Care Med.* **162**, 1553–1560
6. Buckley, C. D., Pilling, D., Henriquez, N. V., Parsonage, G., Threlfall, K., Scheel-Toellner, D., Simmons, D. L., Akbar, A. N., Lord, J. M., and Salmon, M. (1999) *Nature* **397**, 534–539
7. Jeong, J., Han, I., Lim, Y., Kim, J., Parks, I., Wood, A., Couchman, J. R., and Oh, E. S. (2001) *Biochem. J.* **356**, 231–237
8. Kapila, Y. L., Wang, S., and Johnson, P. W. (1999) *J. Biol. Chem.* **274**, 30906–30913
9. Sharma, A., Askari, J. A., Humphries, M. J., Jones, E. Y., and Stuart, D. I. (1999) *EMBO J.* **18**, 1468–1479
10. Aeschlimann, D., and Thomazy, V. (2000) *Connect. Tissue Res.* **41**, 1–27
11. Pereira, M., Rybarczyk, B. J., Odrlic, T. M., Hocking, D. C., Sottile, J., and Simpson-Haidaris, P. J. (2002) *J. Cell Sci.* **115**, 609–617
12. Hocking, D. C., Sottile, J., and Langenbach, K. J. (2000) *J. Biol. Chem.* **275**, 10673–10682
13. Radek, J. T., Jeong, J. M., Murthy, S. N., Ingham, K. C., and Lorand, L. (1993) *Proc. Natl. Acad. Sci. U. S. A.* **90**, 3152–3156
14. Griffin, M., Casadio, R., and Bergamini, C. M. (2002) *Biochem. J. Rev.* **368**, 377–396
15. Fesus, L., and Piacentini, M. (2002) *Trends Biochem. Sci.* **27**, 534–539
16. Haroon, Z. A., Hettasch, J. M., Lai, T. S., Dewhirst, M. W., and Greenberg, C. S. (1999) *FASEB J.* **13**, 1787–1795
17. Johnson, T. S., Skill, N. J., El Nahas, A. M., Oldroyd, S. D., Thomas, G. L., Douthwaite, J. A., Haylor, J. L., and Griffin, M. (1999) *J. Am. Soc. Nephrol.* **10**, 2146–2157
18. Liu, S., Cerione, R. A., and Clardy, J. (2002) *Proc. Natl. Acad. Sci. U. S. A.* **99**, 2743–2747
19. Balklava, Z., Verderio, E., Collighan, R., Gross, S., Adams, J., and Griffin, M. (2002) *J. Biol. Chem.* **277**, 16567–16575
20. Gaudry, C. A., Verderio, E., Aeschlimann, D., Cox, A., Smith, C., and Griffin, M. (1999) *J. Biol. Chem.* **274**, 30707–30714
21. Jeong, J. M., Murthy, S. N., Radek, J. T., and Lorand, L. (1995) *J. Biol. Chem.* **10**, 5654–5658
22. Verderio, E., Nicholas, B., Gross, S., and Griffin, M. (1998) *Exp. Cell Res.* **239**, 119–138
23. Belkin, A. M., Akimov, S. S., Zaritskaya, L. S., Ratnikov, B. I., Deryugina, E. I., and Strongin, A. Y. (2001) *J. Biol. Chem.* **276**, 18415–18422
24. LeMosy, E. K., Erickson, H. P., Beyer, W. F., Radek, J. T., Jeong, J. M., Murthy, S. N., and Lorand, L. (1992) *J. Biol. Chem.* **267**, 7880–7885
25. Gentile, V., Thomazy, V., Piacentini, M., Fesus, L., and Davies, P. J. (1992) *J. Cell Biol.* **119**, 463–474
26. Jones, R. A., Nicholas, B., Mian, S., Davies, P. J., and Griffin, M. (1997) *J. Cell Sci.* **110**, 2461–2472
27. Akimov, S. S., Krylov, D., Fleischman, L. F., and Belkin, A. M. (2000) *J. Cell Biol.* **148**, 825–838
28. Takahashi, H., Isobe, T., Horibe, S., Takagi, J., Yokosaki, Y., Sheppard, D., and Saito, Y. (2000) *J. Biol. Chem.* **275**, 23589–23595
29. Leblanc, A., Day, N., Menard, A., and Keillor, J. W. (1999) *Protein Expr. Purif.* **17**, 89–95
30. Verderio, E., Coombes, A., Jones, R. A., Li, X., Heath, D., Downes, S., and Griffin, M. (2000) *J. Biomed. Mat. Res.* **54**, 294–304
31. De Laurenzi, V., and Melino, G. (2001) *Mol. Cell. Biol.* **21**, 148–155
32. Dedhar, S., Ruoslahti, E., and Pierschbacher, M. D. (1987) *J. Cell Biol.* **104**, 585–593
33. Heath, D. J., Christian, P., and Griffin, M. (2002) *Biomaterials.* **23**, 1519–1526
34. Gronthos, S., Stewart, K., Graves, S. E., Hay, S., and Simmons, P. J. (1997) *J. Bone Miner. Res.* **12**, 1189–1197
35. Woods, A., and Couchman, J. R. (2001) *Curr. Opin. Cell Biol.* **13**, 578–583
36. Gschwendt, M., Dieterich, S., Rennecke, J., Kittstein, W., Muller, H. J., and Johannes, F. J. (1996) *FEBS Lett.* **392**, 77–80
37. Verderio, E., Gaudry, C. A., Gross, S., Smith, C., Downes, S., and Griffin, M. (1999) *J. Histochem Cytochem.* **47**, 1417–1432
38. Lorand, L., and Graham, R. M. (2003) *Nat. Rev. Mol. Cell. Biol.* **4**, 140–156
39. Melino, G., Thiele, C. J., Knight, R. A., and Piacentini, M. (1997) *J. Neurooncol.* **31**, 65–83
40. Upchurch, H. F., Conway, E., Patterson, M. K., Jr., and Maxwell, M. D. (1991) *J. Cell. Physiol.* **149**, 375–382
41. Heath, D. J., Downes, S., Verderio, E., and Griffin, M. (2001) *J. Bone Miner. Res.* **8**, 1477–1485
42. Hasegawa, G., and Saito, Y. (2002) *Minerva Biotechnologica.* **14**, 192
43. Humphries, M. J. (2000) *Trends Pharmacol. Sci.* **21**, 29–32
44. Schlaepfer, D. D., Hauck, C. R., and Sieg, D. J. (1999) *Prog. Biophys. Mol. Biol.* **71**, 435–478
45. Sechler, J. L., Cumiskey, A. M., Gazzola, D. M., and Schwarzbauer, J. E. (2000) *J. Cell Sci.* **113**, 1491–1498
46. Bergamini, C. M., and Signorini, M. (1993) *Biochem. J.* **291**, 37–39
47. Mikula, M., Schreiber, M., Husak, Z., Kucerova, L., Ruth, J., Wieser, R., Zatloukal, K., Beug, H., Wagner, E. F., and Baccarini, M. (2001) *EMBO J.* **20**, 1952–1962
48. Antonyak, M. A., Singh, U. S., Lee, D. A., Boehm, J. E., Combs, C., Zgola, M. M., Page, R. L., and Cerione, R. A. (2001) *J. Biol. Chem.* **276**, 33582–33587

**A Novel RGD-independent Cell Adhesion Pathway Mediated by Fibronectin-bound
Tissue Transglutaminase Rescues Cells from Anoikis**

Elisabetta A. M. Verderio, Dilek Telci, Afam Okoye, Gerry Melino and Martin Griffin

J. Biol. Chem. 2003, 278:42604-42614.

doi: 10.1074/jbc.M303303200 originally published online May 5, 2003

Access the most updated version of this article at doi: [10.1074/jbc.M303303200](https://doi.org/10.1074/jbc.M303303200)

Alerts:

- [When this article is cited](#)
- [When a correction for this article is posted](#)

[Click here](#) to choose from all of JBC's e-mail alerts

Supplemental material:

<http://www.jbc.org/content/suppl/2003/09/03/M303303200.DC2>

This article cites 48 references, 23 of which can be accessed free at

<http://www.jbc.org/content/278/43/42604.full.html#ref-list-1>